# An Agile Single Board Quadrotor Providing ”Eye in the Sky” Capabilities for Marine Environments

Mohammed Raju Hossain, Taufiqur Rahman, Nicholas Krouglicof
Faculty of Engineering & Applied Science
Memorial University of Newfoundland
St. John’s, NL A1B3X5
Email: mrhossain@mun.ca

***Abstract*—This paper presents a robust model independent control method for the stabilization of a four-rotor rotorcraft, which is popularly known as the quadrotor helicopter. In addition, a detailed dynamic model is presented for the formulation of the proposed control law and a prototype platform heavily utilizing printed circuit board technology is proposed for experimentation. This paper focuses on compensating for unknown disturbances (e.g., wind gusts) that naturally occur in a marine environment. In order to employ eye in the sky capabilities in a marine environment, a quadrotor helicopter must hand these disturbances without jeopardizing the stability of the vehicle. To this end, the control law is derived from the Active Disturbance Rejection Control (ADRC) technology, which is reported in the literature to be resistant to external disturbances. The robustness of the proposed controller is demonstrated through numerical simulation of the vehicle's vertical flight. External disturbances in the simulation experiment is considered as a sudden vertical gust of wind acting on the vehicle. In order to quantify the robustness of the controller relative to conventional control technologies, a PD controller under identical flight conditions provides a reference benchmark. The comparative performance of the two controllers shows that the proposed control algorithm significantly outperforms the PD algorithm under the simulated disturbance conditions.**

## I. Introduction

The desire to combine agility, maneuverability and ability to operate in degraded weather conditions with complete autonomy is influencing new requirements for Unmanned Aerial Vehicles (UAV). Among such vehicles, the quadrotor has proven itself to be a promising candidate in terms of the simplicity of its architecture and its capacity to provide improved dynamics. However, a flexible yet robust control scheme that is immune to atmospheric disturbances continues to intrigue researchers [1], [2]. Such a control scheme is of utmost importance, as missions that UAVs have to undertake usually occur in harsh environments, where wind gusts are prevalent (e.g., oceanic wind).

Because agility is a prerequisite for a UAV to overcome wind disturbances, the vehicle must have the dynamic capability to provide agile performance. However, this must be achieved without compromising vehicle stability. Without a suitable control algorithm, it is difficult to completely utilize the dynamic capacity of a vehicle. Hence, it is required to develop an appropriate controller that can deliver faster maneuverability to counteract external disturbances while maintaining stable flight of the vehicle. This demonstrates that there are two requirements for a UAV system for marine environments; namely, a dynamically agile platform and a robust controller that can harness the available dynamics in an effective manner. Accordingly, this paper covers both of these aspects by proposing a vehicle architecture that is expected to provide improved dynamic response. In addition, a robust control algorithm for hovering control of the proposed vehicle is presented.

In order to develop a robust UAV system for marine environments, this paper focuses on designing an agile quadrotor platform with relatively faster and effective dynamic response to environmental disturbances. It was shown experimentally in [3] that agile performance of a quadrotor helicopter can be achieved by scaling down the vehicle platform to attain higher accelerations that allow rapid adaptation to disturbances and results in superior platform stability. This paper accordingly adopts this idea through a monolithic integration of the frame and the actuators (i.e., motor-propeller assembly) of a quadrotor helicopter on a single printed circuit board (PCB). Rhee *et. al.* in [4] showed such an approach where some of the electronics are stacked on the vehicle platform. However, the proposed approach is unique in that it is a true monolithic architecture where all the electronic circuitry is populated on a single PCB. Since a conventional PCB is composed primarily of fibre glass material, a PCB frame provides sufficient rigidity without adding to the weight of the system. This results in an exceptional light weight and low-cost UAV system that is capable of agile performance.

Due to the under-actuated nature of a quadrotor helicopter (i.e., degrees of freedom of the system are greater than the number of actuators), it is difficult to formulate a controller that can operate in a complex aerodynamic environment. Correspondingly, many control algorithms ranging from linear conventional PD (proportional-derivative) control to more advanced non-linear techniques such as backstepping, feedback linearization etc. (e.g., [5], [6]) have been proposed in the literature. However, few from the prior art have considered the influence of unknown atmospheric disturbances on autonomous flight. Correspondingly, this paper focuses on deriving a control algorithm that offers sufficient robustness against atmospheric disturbances. While it is relatively simple to implement classic PID control on embedded electronics, it is susceptible to failure under stochastic disturbances that may occur in a practical application. As an alternative, modern control technologies that generally rely on a mathematical model of the system and the environment can be adopted for robust control performance. However, such a controller

978-0-933957-40-4 ©2013 MTS

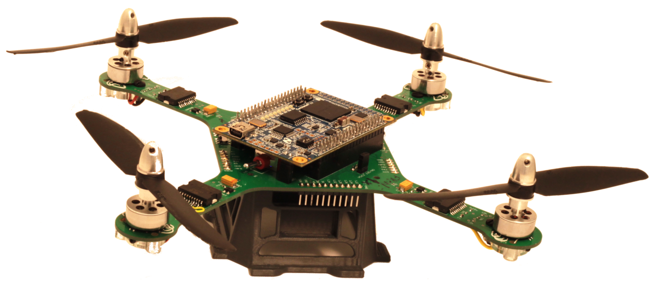

Fig. 1. The proposed quadrotor architecture.

is cumbersome in terms of computational complexity, which renders it unattractive for an embedded application. Hence, a suitable control algorithm for a UAV system must balance two competing constraints of being computationally simple and being resistant to external disturbances. In light of the above discussion, active disturbance rejection control technology [7] offers an attractive solution for control of a UAV system because of its computational simplicity that does not require a model of the system. The fundamental theory of ADRC originates from estimating the system dynamics and disturbances by an external state observer (ESO). The control effort computed by the ADRC algorithm actively compensates for the estimated disturbances and achieves greater disturbance tolerance. Therefore, this paper adopts ADRC technology as the control algorithm for the proposed UAV platform.

In order to elaborate on the aforementioned ideas, this paper is organized as follows. Section II presents the design of the proposed UAV platform. A mathematical model of the UAV platform is formulated in Section III to conduct numerical experiments. A control architecture for a quadrotor helicopter is developed in Section IV. The performance of the adopted controller is assessed in Section V. Finally, Section VI offers concluding remarks and proposes a number of future developments.

## II. Agile Quadrotor Vehicle

### A. The Vehicle Frame

The prototype quadrotor is presented in Fig. 1. The vehicle frame is based on a single PCB that incorporates all necessary avionics, actuators and their drivers. Although the proposed vehicle platform features a monolithic design, an initial prototype of the system employs two PCBs for the sake of development and testing. Accordingly, the controller board sits on top of the main vehicle frame. To generate lift, the vehicle utilizes four fixed pitch propellers with diameter of 5 inches. The normal distance between two motor-propeller assemblies is 10 inches. At the present stage of development, the system weighs 160 gm without battery.

### B. Avionics

A 3-axis magnetometer, a 3-axis accelerometer, and a 3-axis gyroscope serve as the motion sensors for the UAV system. In addition, a 16 MHz Atmel microprocessor was used to

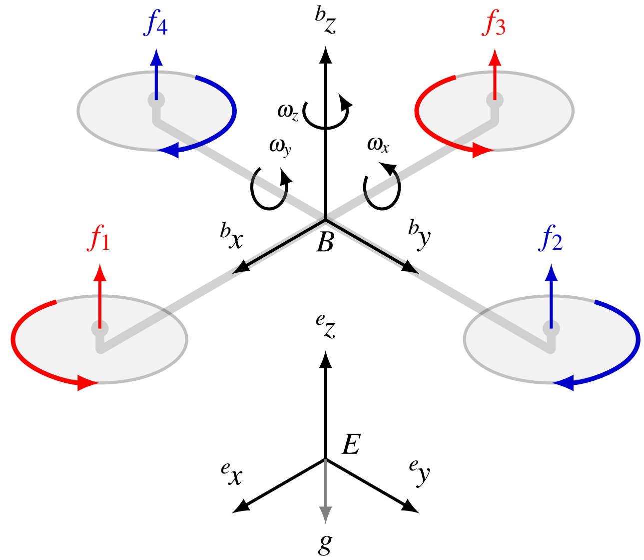


Fig. 2. Free body diagram of a quadrotor.

estimate all the three Euler angles. In this paper, the ZYX rotation convention of Euler angles was adopted. These angles are defined sequentially as: yaw ($\psi$), pitch ($\theta$) and roll ($\phi$). A barometer is used to measure altitude and a commercially available transceiver is employed to communicate with a host computer. The vehicle also incorporates two pairs of MOSFETs based three half H-bridges to drive the motors. The controller board features a Field Programmable Gate Array (FPGA) that generates all the necessary control signals. Exploiting the parallelism of an FPGA chip, it is possible to dispatch control signals to all four actuators without any latency, which is difficult to achieve with conventional microcontroller or embedded computer.

## III. Mathematical Model of the Quadrotor

In general, the mathematical model describing the dynamics of a quadrotor in 3D space is obtained by representing the vehicle as a rigid body. The equations of motion for such a body are provided by Newton-Euler formalism [8] as,

$$\begin{bmatrix} {}^e\boldsymbol{F} \\ {}^b\boldsymbol{M} \end{bmatrix} = \begin{bmatrix} m\boldsymbol{I}_{3\times3} & \boldsymbol{0}_{3\times3} \\ \boldsymbol{0}_{3\times3} & \boldsymbol{I} \end{bmatrix} \begin{bmatrix} {}^e\dot{\boldsymbol{v}} \\ {}^b\dot{\boldsymbol{\omega}} \end{bmatrix} + \begin{bmatrix} \boldsymbol{0}_{3\times3} & \boldsymbol{0}_{3\times3} \\ \boldsymbol{0}_{3\times3} & -\boldsymbol{S}(\boldsymbol{I}\,{}^b\boldsymbol{\omega}) \end{bmatrix}. \quad (1)$$

In (1), the external forces $\boldsymbol{F} \in \Re^3$ are expressed in the inertial frame $E$, and the external moments $\boldsymbol{M} \in \Re^3$ acting on the body are expressed in the body frame $B$. Here, $\boldsymbol{I}_{3\times3}$ is the identity matrix, $\boldsymbol{v}$ is the velocity vector of the body at the center of mass in the inertial frame, $\boldsymbol{\omega}$ is the angular velocity vector of the body expressed in the body frame, $m$ is the mass of the body, $\boldsymbol{I}$ is the inertia matrix with respect to the body frame that coincides with the three principal axes of the body and $\boldsymbol{S}(\cdot)$ is the skew-symmetric matrix.

The vehicle platform is maneuvered by generating control forces from the four rotors, numbered 1 through 4 in Fig. 2, with odd numbered propellers being reverse pitched to the even numbered ones. Due to this counter rotating nature of the opposite propeller pairs, the gyroscopic effects and aerodynamic torques tend to cancel in a near hover flight. Increasing and decreasing the the thrust generated by the four propellers at the same rate permits climbing and descending. This lift $U_1 = \sum_{i=1}^{4} f_i$ is applied along the $z$ axis of the body frame. Here, $f_i$ is the thrust generated by the $i$ propeller. Since the vehicle

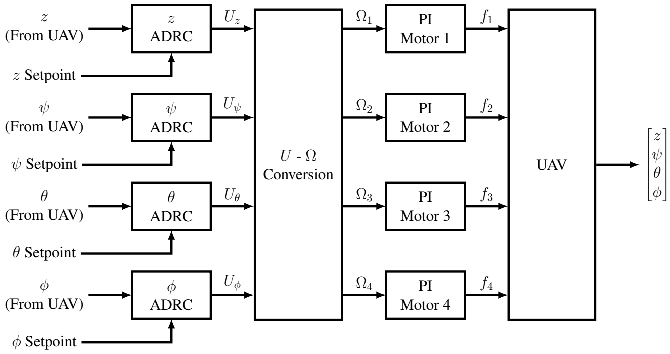


Fig. 3. Proposed control architecture for a quadrotor UAV.

motion is observed from the inertial frame, it is required to transform the motion vectors (i.e., linear and angular velocity) to the frame using a rotation matrix $\boldsymbol{R}$ that provides the relative orientation of the body frame with respect to the inertial frame. In order to create a rolling moment along the $x$ axis of the body frame, thrust from one of the even numbered rotors is increased while the thrust from the other one is decreased simultaneously; i.e., $U_2 = (f_4 - f_2)l$. Here, $l$ is the distance of a rotor from the centre of mass of the body. It should be noted that all four rotors are equidistantly located from the centre of mass. In a similar manner, a pitching moment is obtained using the two odd numbered rotors; i.e., $U_3 = (f_1 - f_3)l$. Finally, yaw motion is performed by increasing the moments of both even numbered rotors while decreasing the moments from the other two; i.e., $U_4 = (m_2 + m_4 - m_1 - m_3)$, where, $m_i$ is the reaction torque created by the $i$ rotor. This external input from the actuators can be expressed as:

$$\boldsymbol{U}(\Omega) = \begin{bmatrix} \boldsymbol{R} & \boldsymbol{0_{3\times 3}} \\ \boldsymbol{0_{3\times 3}} & \boldsymbol{I_{3\times 3}} \end{bmatrix} \begin{bmatrix} 0 & 0 & U_1 & U_2 & U_3 & U_4 \end{bmatrix}^T . \tag{2}$$

The control inputs are the functions of the propeller speeds $\Omega_i$. For the sake of simplicity, a first order DC motor model has been incorporated into the UAV model. Each motor drives a single propeller. The aerodynamic lift force and moments are given by:

$$f_i = T_C\, \Omega_i^2, \quad m_i = D_C\, \Omega_i^2.$$

Here, $T_C$ is the thrust constant and $D_C$ is the drag constant that is empirically determined.

Equation (3) represents the gyroscopic effect in the body frame generated due to the rotation of the propeller and only contributes to the angular motion of the vehicle:

$$^bG = \begin{bmatrix} \boldsymbol{0_{3\times 1}} \\ J_r \begin{bmatrix} -\omega_y \\ \omega_x \\ 0 \end{bmatrix} \sum \Omega_i \end{bmatrix} . \tag{3}$$

Here, $J_r$ is the inertia of the rotors. All the external forces and the moments acting on the quadrotor are modelled in (1), (2) and (3) are algebraically manipulated to obtain (4).

$$\left.\begin{aligned}
{}^e\ddot{X} &= (\sin\phi \sin\psi + \cos\phi \sin\theta \cos\psi)\, \frac{U_1}{m} \\
{}^e\ddot{Y} &= (-\sin\phi \cos\psi + \cos\phi \sin\theta \sin\psi)\, \frac{U_1}{m} \\
{}^e\ddot{Z} &= -g + (\cos\phi \cos\theta)\, \frac{U_1}{m} \\
\dot{\omega}_x &= \frac{I_{yy} - I_{zz}}{I_{xx}}\, \omega_y\, \omega_z - \frac{J_r}{I_{xx}}\, \omega_y \sum \Omega_i + \frac{U_2}{I_{xx}} \\
\dot{\omega}_y &= \frac{I_{zz} - I_{xx}}{I_{yy}}\, \omega_x\, \omega_z + \frac{J_r}{I_{yy}}\, \omega_x \sum \Omega_i + \frac{U_3}{I_{yy}} \\
\dot{\omega}_z &= \frac{I_{xx} - I_{yy}}{I_{zz}}\, \omega_x\, \omega_y + \frac{U_4}{I_{zz}}
\end{aligned}\right\} \tag{4}$$

In (4), $X$, $Y$ and $Z$ denote the position of the body with respect to the inertial frame, while $\psi$, $\theta$ and $\phi$ are the yaw, pitch and roll angles respectively. In addition, $g$ represents the acceleration due to gravity. Finally, in order to generate the control signal $\boldsymbol{U_i}$, a transformation matrix is used that provides the Euler angle rates in terms of the angular velocity vector. Integrating these rates provides the three Euler angles.

## IV. Control Architecture

A generic second order system model is adopted in order to formulate a mathematical framework for ADRC, wherein system dynamics and external disturbances are treated as *total disturbance* [7], [9]:

$$\ddot{y} = f(y, \dot{y}, p) + bu. \tag{5}$$

Here, $f(\cdot)$ is the combined effect of the dynamics of the model and the external disturbances $p$. In general, $f(\cdot)$ is a non-linear function of $p$. In (5), $u$ is the control input, $y$ is the measured output, and $b$ is a system parameter. It should be noted that $f(\cdot)$ need not be known explicitly for ADRC, only an estimation provided by an extended state observer is sufficient. Equation (5) can be formulated as a state-space system by augmenting an additional state $\dot{z}_3 = \dot{f}$, as shown in (6).

$$\left.\begin{aligned}
\dot{x}_1 &= x_2 \\
\dot{x}_2 &= x_3 + bu, \quad x_3 \triangleq f(y, \dot{y}, p) \\
\dot{x}_3 &= \dot{f}(\cdot) \\
y &= x_1
\end{aligned}\right\} \tag{6}$$

Here, $x_3$ is the total disturbance that is unknown and can be estimated using an external state observer (7) proposed by Prof. Han [7].

$$\left.\begin{aligned}
e_0 &= y - z_1 \\
\dot{z}_1 &= z_2 + \beta_1 e_0 \\
\dot{z}_2 &= z_3 + \beta_2 e_0 + \hat{b}u \\
\dot{z}_3 &= \beta_3 e_0
\end{aligned}\right\} \tag{7}$$

In (7), $e_0$ is the observer error, $\beta_1$, $\beta_2$, $\beta_3$ are the observer gains, $\hat{b}$ is the estimated value of $b$, $z_1$, $z_2$ and $z_3$ are observer states tracking $y$, $\dot{y}$ and $f(\cdot)$ respectively. In this case, $z_3$ is the extended state and a PD controller is designed to control the platform by rejecting the disturbance in real time:

$$\left.\begin{aligned}
u &= \frac{u_0 - \hat{f}}{\hat{b}} = \frac{u_0 - z_3}{\hat{b}} \\
u_0 &= k_p(r - y) - k_d \dot{y}
\end{aligned}\right\} \tag{8}$$

In (8), $r$ is the desired system output, $u_0$ is the virtual control signal which undergoes disturbance rejection before generating an actuation signal for the plant.

In the case of a quadrotor, four different ESOs were implemented to estimate the disturbances in altitude, roll, pitch and yaw measured

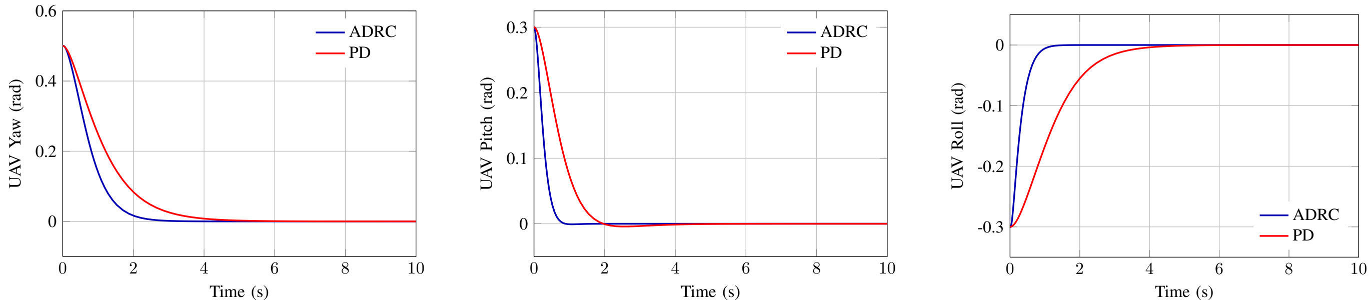


(a) Yaw

(b) Pitch

(c) Roll

Fig. 4. Orientation stabilization under disturbances.

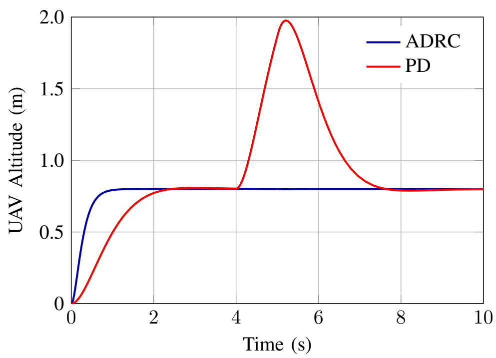


Fig. 5. Controlled altitude response of the vehicle under disturbance.

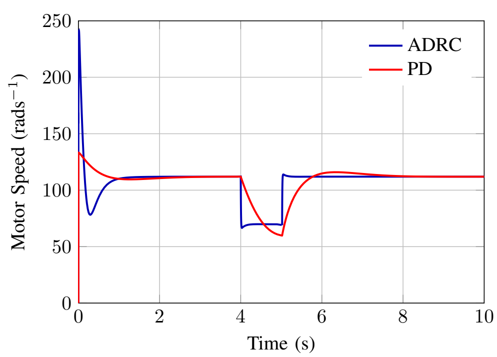


Fig. 6. Controlled speed of a representative propeller.

from the quadrotor plant model. The disturbances are then rejected using the linear PD formulation in (8). In order to demonstrate the disturbance rejection performance of ADRC, a classical PD controller was also implemented as a reference:

$$u = k_p(r - y) - k_d\dot{y}. \tag{9}$$

It can be seen that the only difference between ADRC and PD in this case is, ADRC is capable of real time estimation and rejection of environmental disturbances, whereas a classical PD controller has no such capacity.

## V. Parameter Tuning and Simulation

A numerical simulation experiment was conducted to assess the performance of the proposed control law against classical PD technology with the following simulated environment conditions and initial state of the UAV:

- The quadrotor is controlled from an unstable initial condition as defined by roll($\phi \neq 0$), pitch($\theta \neq 0$) and yaw($\psi \neq 0$). Specifically, the simulation experiment starts from the following initial conditions: $Z = 0$ m, $\phi = -0.3$ rad, $\theta = 0.3$ rad, and $\psi = 0.5$ rad. The desired final conditions are: $Z = 0.8$ m, $\dot{Z} = 0$ ms$^{-1}$, $\phi = \theta = \psi = 0$ rad, $\dot{\phi} = \dot{\theta} = \dot{\psi} = 0$ rads$^{-1}$.
- The performance of the controllers is recorded under a vertical gust wind disturbance acting along the positive $z$ axis of the inertial frame, which is provided by a square function that sustains from $t = 4.0$ s to $t = 4.5$ s and has an amplitude 6 ms$^{-1}$.
- Disturbance is applied while the vehicle is stabilized; i.e., $\phi \approx \theta \approx 0$. It should be noted that the yaw angle $\psi$ is not critical to vehicle stability.

Fig. 5 presents the comparative performance of the two controllers for altitude response in the presence of a disturbance. Observe that, the ADRC control algorithm efficiently attenuates the induced external velocity, whereas PD fails to maintain the UAV altitude effectively. The reaction of the quadrotor to the external disturbance is exhibited by an impulse vertical force that attempts to increase the altitude of the system. In order to counteract this effect, the controller must reduce the propeller speeds accordingly so that it can maintain the desired altitude. It can be seen in Fig. 6 that the ADRC controller almost instantaneously responded to the external disturbance. In contrast, the PD controller exhibit a slower response that resulted in a large departure from the desired altitude.

Fig. 4 shows the stabilization control performance in terms of the orientation of the vehicle. Since the vehicle starts from an unstable state, both controllers attempt to stabilize the vehicle by manipulating the Euler angles to zero. The ADRC algorithm shows a faster settling time relative to the PD controller with little or no overshoot. The ADRC framework allows for aggressive tuning of the controller while maintaining stable performance. In the experiment, it was seen that aggressive tuning of the PD controller forces the vehicle out of the stable operating region. Hence, it was tuned moderately, which resulted in slower stabilization of the vehicle.

It needs to be noted that both controllers were tuned to their best performance in the simulation experiment. Admittedly, it cannot be claimed that the controllers were tuned optimally, since the tuning task was a trial and error exercise. However, the significantly inferior performance exhibited by the PD controller under external disturbances (see Fig. 5) cannot be attributed to suboptimal tuning only. While it is possible to obtain better performance from the PD controller using a more elaborate tuning scheme, it is unlikely that it will outperform the ADRC controller, which is also tuned by trial and error.

Relative to the PD controller, a large set of parameters were required to tune the ADRC controller. However, a parameterization technique proposed in [10] can be employed to tune these parameters. Accordingly, the observer gains and controller gains are selected as follows:

$$\beta_1 = 3\omega_0,\ \beta_2 = 3\omega_0^2,\ \beta_3 = \omega_0^3,\ k_p = \omega_c^2,\ k_d = 2\omega_c, \qquad (10)$$

where, $\omega_0$ and $\omega_c$ are the observer bandwidth and controller bandwidth respectively. These parameters along with $\hat{b}$ in (7) are found by a trial and error exercise.

## VI. CONCLUSION & FUTURE WORKS

### A. Conclusion

In this paper, a quadrotor design was presented that is capable of operating in a marine environment while withstanding atmospheric disturbances. This has been achieved by proposing a monolithic design of the vehicle, which can potentially provide agile performance in a small and cost effective form factor. In addition, an existing control technology (i.e., ADRC) was adopted for the proposed system. It was shown through simulation experiment that the ADRC controller outperforms a classic PD controller in terms of disturbance suppression. The ADRC controller is particularly well suited for an embedded application where available computing resources are limited. Since it does not require a computationally complex model of the system for its operation, a practical implementation is resource efficient. Hence, this controller can provide robust performance without requiring large computation resources.

### B. Future Works

In this work, only hovering is focused on since the quadrotor is designed for indoor testing at the present stage of development. Because of the GPS denied nature of the testing environment, lateral position control of the system was not implemented. Correspondingly, a GPS can be incorporated into the avionics of the vehicle for lateral position control, homing etc. In addition, a comprehensive wind disturbance model can improve the accuracy of the simulation. In particular, models for lateral wind disturbance need to be developed to validate the performance in the presence of naturally occurring disturbances such as wind gusts.

## REFERENCES


[1] A. Martin and G. Abba, "Robust nonlinear controls of model-scale helicopters under lateral and vertical wind gusts," *IEEE Transactions on Control Systems Technology*, vol. 20, no. 1, pp. 154–163, 2012.

[2] G. Nikolakopoulos and A. Tzes, "Constrained-control of a quadrotor helicopter for trajectory tracking under wind-gust disturbances," *15th IEEE Mediterranean Electrotechnical Conference*, pp. 1411–1416, 2010.

[3] A. Kushleyev, V. Kumar, and D. Mellinger, "Towards a swarm of agile micro quadrotors." in *Robotics: Science and Systems*, 2012.

[4] S. H. Rhee and Y. S. Lee, "Unmanned flying vehicle made with pcb," Nov. 29 2010, US Patent App. 12/954,975.

[5] T. Madani and A. Benallegue, "Backstepping control for a quadrotor helicopter," in *Intelligent Robots and Systems, 2006 IEEE/RSJ International Conference on*, 2006, pp. 3255–3260.

[6] S. Al-Hiddabi, "Quadrotor control using feedback linearization with dynamic extension," in *Mechatronics and its Applications, 2009. ISMA '09. 6th International Symposium on*, 2009, pp. 1–3.

[7] J. Han, "From pid to active disturbance rejection control," *Industrial Electronics, IEEE Transactions on*, vol. 56, no. 3, pp. 900–906, 2009.

[8] D. C. Karnopp, D. L. Margolis, and R. C. Rosenberg, *System Dynamics: Modeling, Simulation, and Control of Mechatronic Systems*. Wiley. com, 2012.

[9] Z. Gao, Y. Huang, and J. Han, "An alternative paradigm for control system design," *Decision and Control, 2001. Proceedings of the 40th IEEE Conference on*, vol. 5, pp. 4578–4585, 2001.

[10] Z. Gao and G. Tian, "Extended active disturbance rejection controller," Apr. 24 2009, WO Patent 2,009,051,891.